RSC Advances

ROYAL SOCIETY OF CHEMISTRY

www.rsc.org/advances

RSC Advances

RSCPublishing

Article

Investigation on Antifouling Universality of Polyvinyl Formal (PVF) Membranes Utilizing Atomic Force Microscope (AFM) Force Curves

Cite this: DOI: 10.1039/x0xx00000x

Received ooth January 2015,
Accepted ooth January 2015

DOI: 10.1039/x0xx00000x

www.rsc.org/

Yunqiang Liu [a], Linyan Xu [a*], Yunpeng Song [a], Xing Fu [a], Jing Zou [a], Xiaotang Hu [a], Zhongyi Jiang [b], Xueting Zhao [b]

As a nano-Newton level force sensor, AFM probe with a protein-modified tip could be used to investigate the antifouling property of different ultrafiltration membranes. In this paper, the spring constants of the cantilevers of AFM probes were calibrated with a SI-traceable measurement system consisting of a precision balance, an optical lever and nano-positioning stages. The calibration system for the measured AFM cantilevers has less than 3% uncertainty, highly narrowing the large range given by the distributers. Thus, the adhesion forces between the AFM probes with different immobilized proteins and various ultrafiltration membranes could be compared with each other using force curves. The antifouling universality of a specific membrane (polyvinyl formal, PVF) towards multiple proteins (bovine serum albumin, lysozyme, catalase and fibrinogen) could be studied comprehensively. The results reveal that the antifouling property of membranes becomes better through blending F127 with PVF for all four foulants, so the antifouling universality of the membrane was improved effectively. The membrane with 60% F127 addition had the best antifouling property. The comparison experiments of protein absorption and water contact angle have also been done. As the F127 additive varied from 0% to 60%, the amount of the protein adsorption on the surface of the membranes decreased significantly and the water contact angle decreased from 58.6 ° to 47.1 °, which indicated that the blend membranes had better antifouling universality. The experimental results were agreed with AFM force curve experiments very well.

1. Introduction

Membrane fouling is a major obstacle to the efficient application of membrane technology.[1,2] Fouling is the deposition and adsorption of the retained particles, colloids, macromolecules, salts, etc., on the membrane surface or on the pore walls. The foulants not only physically interact with the membrane surface but also chemically degrade the membrane materials,[3] leading to a rapid flux decline and a reduced life span of the membranes. It is well-known that increasing the hydrophilicity of the ultrafiltration membrane surface can effectively minimize the protein adsorptions and prevent the membrane fouling. Various methods, such as surface coating,[4] surface grafting,[5,6] and surface segregation[7-10] have been reported in the literatures to increase the surface hydrophilicity of membranes. However, both the surface coating and grafting strategies may narrow the membrane pores, leading to a reduced permeability.[11] In addition, foulant accumulation on pore walls could hardly be solved using these surface modification methods. Therefore, chemical modification method as a promising alternative approach shows its advantages in not suffering from these shortcomings.[12] In the application of membrane, antifouling property was always critical for several different foulants. So the investigation on antifouling universality is necessary and important and the new approach to estimate the antifouling universality of membrane needed to be proposed.

The general aim to construct a hydrophilic membrane surfaces was to resist the interactions between the foulants and the membrane surfaces, such as the electrostatic interaction, the van der Waals interaction, the hydrophobic interaction, and the hydrogen interaction. Foulant-membrane interaction determines the initial foulant adsorption, which plays a dominant role in the development of membrane fouling.[13,14] Static protein adsorption and dynamic ultrafiltration experiments are widely utilized to assess the antifouling performance of the ultrafiltration membranes, which are still known as indirect and macroscopic evidences, however. The adhesion force measurements of the foulant-membrane interaction can provide direct evidences of the antifouling performance of the ultrafiltration membranes. AFM force curve is a good approach to research the interaction between the particles on the tip apex and the sample surface, and to research the mechanical properties further.[15-17] Comparing to other methods, AFM force curve is more direct and sensitive to evaluate the antifouling performance of the membranes with a modified tip. Presently,

an approach utilizing AFM force curve with a bovine serum albumin (BSA) protein immobilized tip to investigate the antifouling performance of the ultrafiltration membranes (PVDF with different additives) has been proposed.[18-20] In fact, it is impossible to study the antifouling property of a membrane towards various proteins with this method. Because a large uncertainty (about 80%) was existed in AFM force curve measurement due to the wide range of the spring constant of the AFM cantilevers with the same model number (from 0.03 N m^{-1} to 0.2 N m^{-1} for CSG10, NT-MDT Corp., Russia) provided by the distributer. So only the data of the adhesion forces from just the same one cantilever is comparable. Thus, the antifouling universality of a membrane versus various foulants will not be comparatively analyzed based on the AFM force curve method without the known spring constants of several cantilevers to be immobilized with a type of foulant on each tip. To systematically study the antifouling universality of the membranes, the calibration of the AFM cantilever must be done before the force curve measurement.

In this study, AFM force curve analysis was employed as a universal technique to evaluate the antifouling universality of the ultrafiltration membranes. A series of polyvinyl formal (PVF) membranes with different percent of additive F127 were prepared via non-solvent induction phase separation process. As one of the polyvinyl alcohol acetal derivatives, PVF not only retained the hydrophilic characteristic, good physical and chemical stability of polyvinyl alcohol, but also exhibited good membrane-forming properties to prepare hydrophilic ultrafiltration membrane due to the introduction of hydrophobic groups.[21,22] Amphiphilic Pluronic copolymer, i.e. F127, was usually used as a surface segregation additive to construct a hydrophilic brush layer on the membrane surface and to further improve the antifouling performance of the membranes.[23,24] Four typical model proteins (BSA, lysozyme, catalase and fibrinogen) are immobilized to the AFM tips to measure the antifouling universality of the membranes. The adhesion forces between the blend membranes with different proteins on the AFM tips are measured in order to compare the antifouling property of the membranes. The adhesion forces between the PVF membranes with different ratios of F127 additive were measured in order to find out the optimal proportion of the additives.

2. Experiments

2.1 Materials

Polyvinyl formal (PVF, MW = 35 kDa, acetalization degree = 80%) purchased from Tokyo Chemical Industry Corp. (Japan) was dried at 60℃ for 12 h before use. Triblock copolymer Pluronic F127 (EO100-PO65-EO100) with Polyethylene oxide (PEO) content of 70 wt% was purchased from Sigma Chemical Company (USA). BSA, lysozyme, catalase and fibrinogen were purchased from Institute of Hematology, Chinese Academic of Medical Sciences (China). 3-aminopropyltriethoxysilane was purchased from Heowns Biochem LLC. (China). Other chemicals were purchased from Kewei Chemicals Corp. (China).

2.2 Preparation of PVF/Pluronic F127 membranes

Membrane casting solutions was prepared by dissolving PVF, and Pluronic F127 in Dimethyl sulfoxide (DMSO). The formulations of the casting solutions were given in Table 1. PVF (14 wt % in the membrane casting solution) was the membrane matrix, Pluronic F127 was the membrane modifier, and DMSO was the solvent. The mixture was stirred at 60℃ for 5 h. After the homogeneous solutions were obtained, the casting solutions were left for 5 h allowing the complete release of bubbles. The solutions were cast on glass plates with a steel knife, and then immersed in a coagulation bath of deionized water (25 ℃). Subsequently, the pristine membranes were peeled off and washed thoroughly with the deionized water to remove the residual solvent. The as-prepared membranes had a wet thickness of about 240 μm and kept in the deionized water before use. The highest ratio of WF127/WPVF is 60%, otherwise the insoluble phenomenon would occur.

Table 1. The formation of casting solutions for preparation of the PVF/Pluronic F127 membranes.

Membrane	Composition of casting solution			W_{F127}/W_{PVF}(%)[a]
	PVF (g)	F127 (g)	DMSO (g)	
1#	1.40	—	8.60	0
2#	1.40	0.14	8.46	10
3#	1.40	0.28	8.32	20
4#	1.40	0.56	8.04	40
5#	1.40	0.84	7.76	60

[a] The weight ratio of Pluronic F127 to PVF in the membrane casting solution.

2.3 Calibration of AFM cantilever

The spring constant of AFM cantilever is of great significance to nano-force measurement.[16,25-27] But the nominal spring constants provided by the manufacturers usually have a relatively large uncertainty since they are the theoretical calculation results based on the designed geometric dimensions and the estimated material parameters, which may deviate from the true values. Therefore, the calibration of AFM cantilever is a necessary produce before it is used for AFM force curve measurement. Among various calibration methods, the way of using electromagnetic balance is believed to be the most reliable one since it is traceable to the International System of Units (SI).[28,29] As schematically illustrated in Fig. 1, the experiment facility we set up consists of a commercial electromagnetic balance (SE2, Sartorius AG Corp., Germany), a home-made AFM head and a group of assistant nano-positioning stages.[29,30]

Four commercial AFM probes (CSG10, NT-MDT Corp., Russia) were calibrated in this work. The nominal value of the spring constant is 0.12 N m^{-1} with a distribution range of 0.03 N m^{-1}~0.2 N m^{-1} according to the datasheet from the distributers. The forces applied to the tips were recorded by the electromagnetic balance and the deflections of the cantilever were recorded by the position sensitive detector (PSD).

The normal spring constant k_N was simply determined by the ratio of the loading force to the deflection as illustrated in Equation (1).

$$k_N = \frac{\Delta m \cdot g \cdot S_D}{\Delta U_y} \quad (1)$$

Here, Δm is the total load increment detected by the balance during the approaching process; ΔU_y is the corresponding voltage shift of the PSD output in the vertical direction; g = 9.80106 m s^{-2}, is the acceleration of gravity in Tianjin, China; S_D is the sensitivity the optical lever consisting of the AFM cantilever, the reflectors and the PSD.

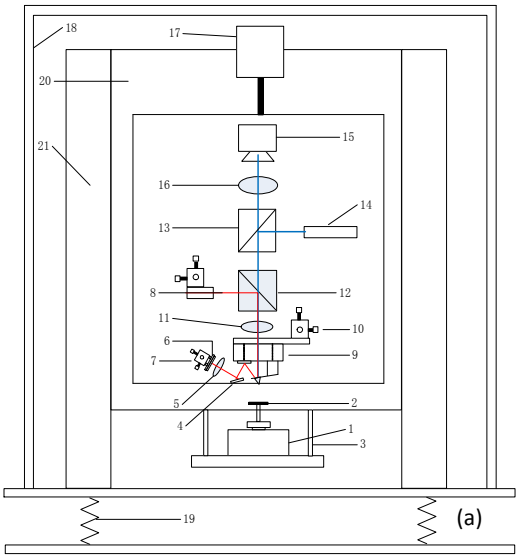

Fig. 1 (a) Schematically illustration of the spring constant calibration system. 1. Electromagnetic balance; 2. Sapphire plate; 3. Balance bracket; 4. Reflector; 5. Lens; 6. PSD; 7, 10. Ultra-precision 3D motor stages; 8. Laser diode; 9. Z-scanner; 11. Objective; 12, 13. Beam splitters; 14. Illuminator; 15. CCD; 16. Tube lens; 17. Z-axis motor stage; 18. Enclosure; 19. Vibration isolator; 20. Supporting breadboard; 21. Supporting columns. (b) Photo of the calibration system.

2.4 Interaction force between membrane surface and protein-immobilized tip

2.4.1 Protein-immobilized AFM tips

Before AFM force curve measurement, the AFM tip was modified according to the procedures described elsewhere.[31] Four Si_3N_4 probes (CSG10, NT-MDT Corp., Russia) calibrated in Section 2.3 were treated with oxygen plasma (150 W, 60 s) and the vacuum of oxygen plasma is about 10^{-5} Pa. Then the probes were chemically modified with 10 mM 3-aminopropyltriethoxysilane toluene solution for 2 h at room temperature. This amine-terminated AFM tip was further reacted with glutaraldehyde (50% in H_2O) for 30 min, which was followed by the reaction with the protein BSA in phosphate buffer solution (PBS, pH = 7.4) for 40 min. Then, the probe was washed with PBS and subsequently stored in PBS. The other three types of proteins (lysozyme, catalase and fibrinogen) were also treated the same way. The immobilized probes should be stored in an icebox in order to retain the activity of the proteins. Before and after the force curve measurement, SEM analysis of the tips was done to ensure the immobilizing and the stability of the proteins.

2.4.2 AFM force curve measurement of membranes

Interaction forces between the ultrafiltration membrane surface and protein-immobilized tips were measured by an atomic force microscope (Multimode IIIa, Bruker Corp., Germany) in the air. The calibration of the spring constant of every cantilever must be done before AFM force measurement of membranes, otherwise the measurement data of different tips could not be compared and analysed.

According to the manual of AFM, the sensitivity of optical lever S_D should be calibrated before AFM force curve measurement. Sensitivity represents the cantilever deflection signal ΔZ_0 from PSD versus the voltage ΔU_0 applied to the piezo scanner in the vertical direction, which can be illustrated by Equation (2).

$$S_D = \frac{\Delta Z_0}{\Delta U_0} \quad (2)$$

In order to avoid the error introduced in the sample deformation, a sample much stiffer than the tips, such as sapphire, was used to calibrate the sensitivity. The sensitivity will change with different cantilever geometric dimensions, and will also change with the position and quality of the laser spot on the cantilever. Therefore, the installation position of a tip and the laser spot should not be moved during the whole calibration process in order to avoid the changes of the sensitivity.

According to the specialty of AFM force measurement, the procedure is designed as follows. Firstly, the spring constants of four cantilevers were calibrated with the balance method in Section 2.3, respectively. Secondly, every tip was immobilized with different protein according to the method mentioned in Section 2.4.1. Thirdly, one tip was installed and its sensitivity was calibrated with a sapphire sample. Fourthly, 1# membrane was mounted on the sample stage of AFM for the adhesion force measurement. As the membrane surface approached the tip, an interaction was occurred between the tip and the membrane surface, which induced a deflection of the cantilever. By multiplying the spring constant by the deflection of the cantilever and introducing Equation (2) here, the force F between tip and membrane surface could be calculated by Equation (3).

$$F = k_N \cdot \Delta Z = k_N \cdot S_D \cdot \Delta U \quad (3)$$

Here, ΔZ represents the deflection of the cantilever; ΔU represents the PSD output voltage of the cantilever, which could be derived from the data in the vertical axis of the AFM force curve.

The adhesion force experiment between an AFM tip without protein treatment and PVF membrane 1# was done at the beginning. Then the results can be compared with AFM tips after protein treatment, which aim at being another proof of AFM tip modification. The adhesion force could be detected in the same manner when the surface was retracted from the tip.

An extending-retracting curve then could be recorded from these measurements. Then, the other membranes (2#, 3# and 4#) were measured in turns. Pay attention to keep the optical level and the probe immoveable during samples replacement. Finally, the other three tips were replaced in turns and the experiments repeated. A speed of 0.1 μm s^{-1} was applied to obtain all the force curves. Approximately 50 extending/retracting cycles were performed for each membrane surface versus one tip and they were collected from at least five positions on the same sample. That is to say, for four tips and five sample membranes, 1,000 force measurements were done is this part.

2.5 Protein adsorption and water contact angle on PVF/F127 membrane

Here, the experiments of protein adsorption and water contact angle were also done to evaluate the antifouling performance of ultrafiltration membranes. Then these results were compared with AFM force curve method in order to verify the measurement accuracy of the antifouling universality.

The membranes were cut into a round shape with 3 cm diameter and the surface area was about 7 cm^2. The membranes were put into vials containing 5 mL of 1.0 mg mL^{-1} protein solutions of BSA, lysozyme, fibrinogen and catalase, respectively. The pH value of the solutions was kept at 7.0 with 0.1 M phosphate buffer solution and incubated at 25℃ for 24 h to reach equilibrium. The concentrations of protein in the solution before and after contact with the membranes were measured with a UV-VIS spectrophotometer (UV-2800, Hitachi Corp., Japan). Then a noticeable adsorbed protein amount was measured.

The surface wettability of PVF and PVF/F127 blend membranes was evaluated by the water contact angle experiments using a goniometer (Erma Contact Angle Meter, Japan). The measurements were taken at five different locations on the same sample, and the average value of the experimental results was calculated afterwards.

3. Results and discussion

3.1 Spring constant calibration of cantilevers

Using the system of AFM cantilever calibration based on balance method, the spring constant were measured with small residual errors and good repeatability. Fig. 2a shows the linearity of spring constant of BSA cantilever and the residual errors. The horizontal axis represents the displacement of the nano-positioning stage in the Z direction, and the vertical axis represents the force between the tip and the membrane. There were ten steps in a load cycle of the measured cantilever. The curve of the force to the displacement of every cycle was linearly fitted. The maximum of residuals in the full scale (0.34 μN) was 2.8%, which could be used to describe the nonlinearity. Thus, it is reliable to use the slope of the curve as the spring constant. Fig. 2b shows the repeatability of the spring constant of BSA cantilever and its relative deviation. Ten repeated load cycles were carried out and the mean value of the slopes of the curves was calculated as the spring constant of cantilever. During the calibration process, the voltage from PSD in lateral direction maintains constant, which means torsion did not happen to this cantilever. The other results of calibration are shown in Table 2.

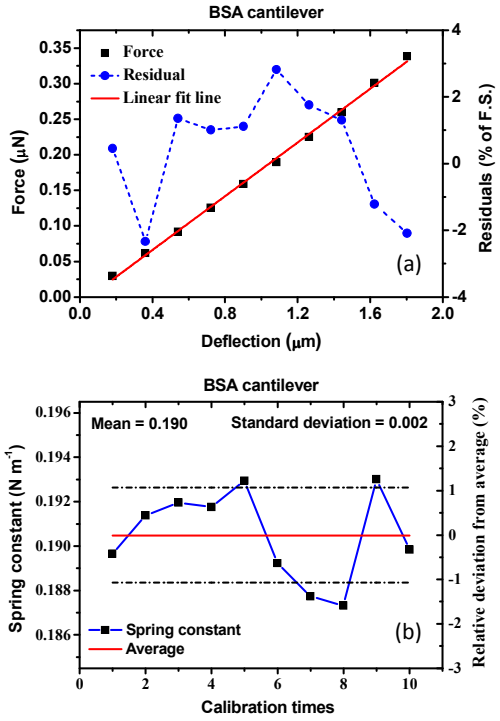

Fig.2 Calibration results of the spring constant of the BSA cantilever. (a) Linearity measurements; (b) Repeatability measurements.

Table 2 Calibration results of four cantilevers

cantilever	Protein immobilized	Spring constant(N m^{-1})	Residuals (%)
1#	BSA	0.190	2.8
2#	Lysozyme	0.126	2.6
3#	Catalase	0.090	1.9
4#	Fibrinogen	0.114	2.2

3.2 Interaction force between membrane surface and protein-immobilized tip

3.2.1 Protein-immobilized AFM tips

Fig. 3 shows the SEM images of BSA-immobilized AFM tip. It can be seen that BSA proteins have been aggregated into small clusters, and then many clusters are immobilized to the tip and also the cantilever. Comparing to other places on the cantilever, there are more protein clusters gathered on the tip. In comparison, there is no much difference in the pictures before and after the force curve experiments. The protein clusters were well-fixed on the AFM tip. That is to say, the whole force curve measurements were not influenced by the proteins on the tip, and the adhesion forces calculated from different force curves could be compared with each other.

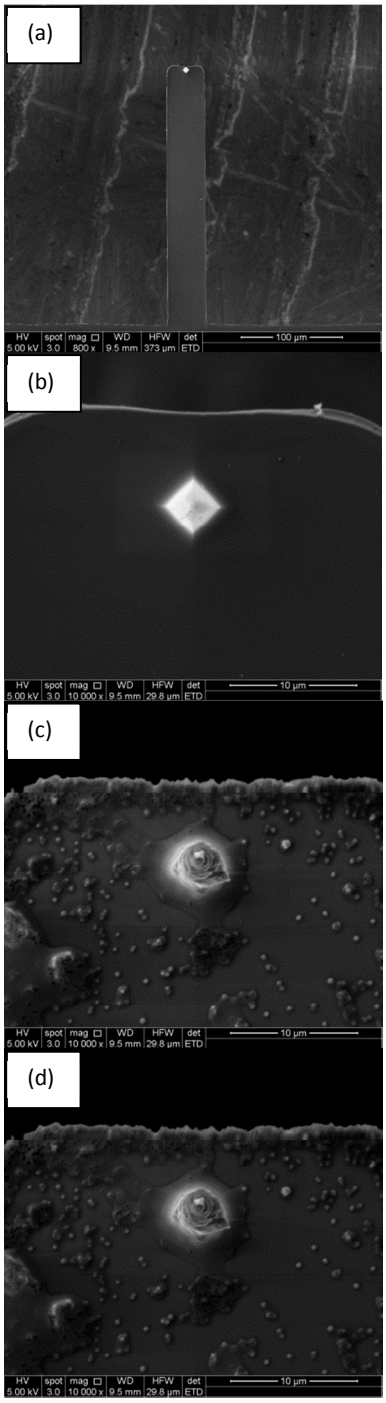

Fig. 3 SEM images of the AFM tip. (a) Tip and cantilever; (b) Tip before protein treatment; (c) Tip after protein treatment; (d) Tip after force-curve experiment.

3.2.2 AFM force curve measurement of membranes

Because membrane fouling originates from the accumulations and adsorptions of foulants on the membrane surfaces, the antifouling performance of the membranes is dominated by the interaction between the foulants and the membrane surfaces. Adhesion force measurements by AFM are presented to support the antifouling mechanism of the membranes. And previous results demonstrated by others have also shown that the magnitude of the adhesion force correlates closely with the fouling propensity of the membranes and the surfaces in the presence of organic foulants.[32-36] The original force curve of AFM describes the change of PSD output voltage when the tip approaches, bends and retracts towards the membranes. The adhesion force was calculated by Equation (3). Fig. 4a~e shows the interaction force between BSA-tip and the PVF membranes with 0 ~ 60 percentage of F127 additive. X-axis represents the displacement of the AFM piezo scanner in the vertical direction, and Y-axis represents the interaction force between the tip and the membrane. There is a little inflexion point in the extending curve, which is induced by the abrupt attraction between the tip and the membrane. Then in the retracting curve, an obvious inflexion point appears when the tip break free of the attraction. The inflexion point in the retracting curve indicates the adhesion force between the tip and the membranes, and it is used to evaluate the antifouling performance of the membranes. Experimental results suggest that the PVF/F127 membrane showed better antifouling properties than pristine PVF membrane. With the increasing of F127 additive percentage, the antifouling performance became more effective. From the data error bar of 50 repeated measurements for each probe recorded in fig. 4f, it was suggested that the data with larger adhesion force has a relatively large uncertainty.

Adhesion force experiment (fig. 4g) between an AFM tip without protein treatment and PVF membrane was done before fig. 4a~e. The force was much smaller than that of protein-immobilized tip in the magnitude.

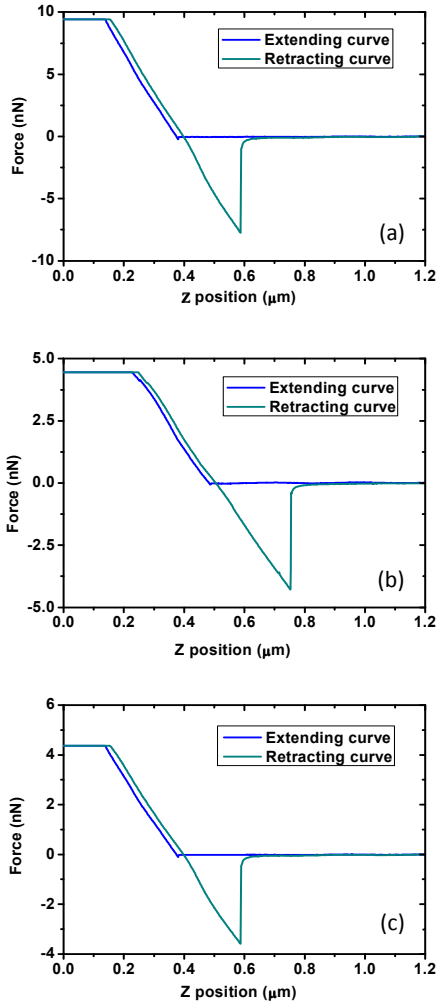

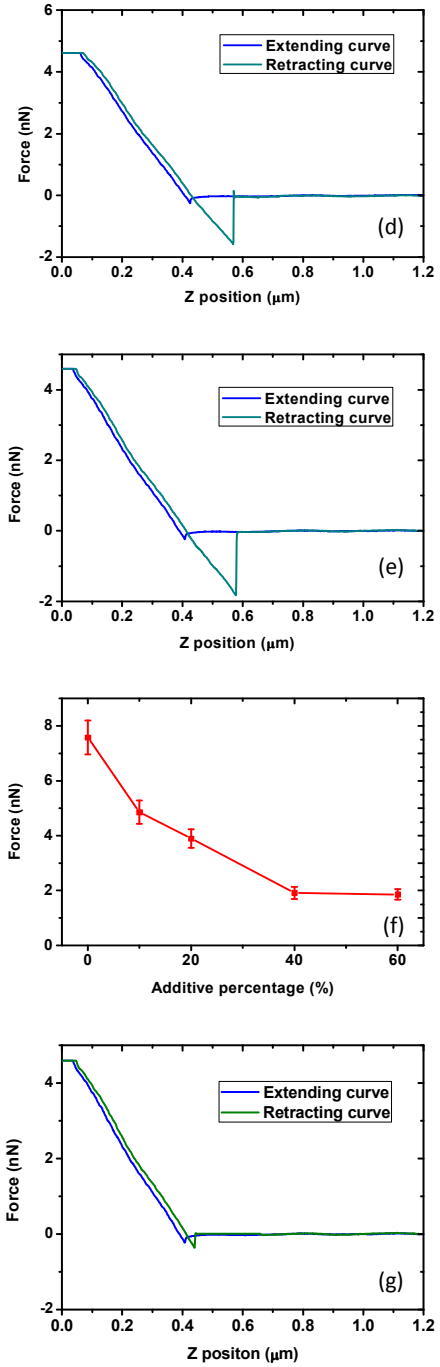

Fig. 4 Force-curve records of BSA tip against (a) PVF membrane, (b) 10% additive F127, (c) 20% additive F127, (d) 40% additive F127, and (e) 60% additive F127. (f) Sum up of the adhesion forces with error bars. (g) Force-curve records of AFM tip without protein against PVF membrane.

Adhesion force experiment was also made between the other three model proteins (lysozyme, catalase and fibrinogen) and the five different membranes. The main purpose of these experiments is to compare the antifouling performance of the membranes against different proteins, and to study the antifouling universality of the membranes. Fig. 5 shows the adhesion force between the four model proteins and the five different membranes. The results implied that additive F127 had better antifouling universality. PVF with F127 additive had a relatively smaller adhesion force to all four model proteins. It was reported that the elimination of membrane foulant adhesion was the key factor in controlling membrane organic fouling.[13] As a result, the antifouling universality of membrane can be a reference of designing membranes.

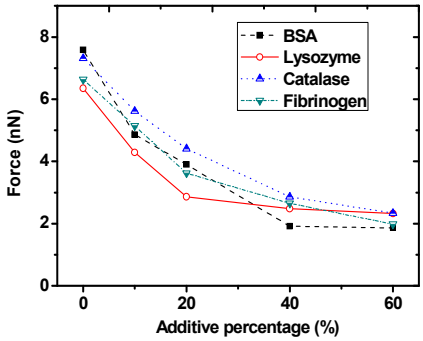

Fig. 5 Adhesion force between four typical proteins and the PVF/F127 membranes with different ratios (0, 10%, 20%, 40%, 60%).

The interaction between the membrane surfaces and the model proteins had a substantial impact on the membrane fouling. Pluronic F127 bearing hydrophilic PEO segments and hydrophobic PPO segments was considered as both excellent surface antifouling modifier.[23,37] The hydrophilic PEO blocks could freely aggregated on the membrane surface to form a compact antifouling brush layer that effectively helped the decrease of the non-specific interaction forces between the model proteins and the membranes. The PVF/F127 membrane successfully reduced the affinity for model proteins. The significant decrease in the adhesion force may originate from the energetic adhesion barrier created by the extended antifouling brushes on the membrane surfaces. Moreover, higher F127 contents in membranes indicated high surface coverage of PEO segments on membranes, which resulted in the minimum adhesion force and an improved antifouling property.

3.3 Water contact angles and Protein adsorption on PVF/F127 membranes

Water contact angle measurement and protein adsorption measurement were common methods to evaluate the antifouling performance of the membranes. Fig. 6 shows the water contact angles of PVF/F127 membranes. The hydrophilicity of PVF/F127 membrane surfaces was characterized by water contact angle measurements. The PVF membrane possessed the highest water contact angle of 58.6 °, while the PVF/F127 membranes had lower water contact angles. With the increasing of the F127 additive percentage, the water contact angles were remarkably decreased to 47.1 °. This suggested the coverage of PEO segments on the membrane surfaces became higher as the concentrations of F127 increased. It was well known that membranes with higher hydrophilicity exhibited better antifouling property. Comparing to Fig. 4f, the results also showed the equivalent tendency the of antifouling performance. The protein adsorption was also carried out to evaluate the antifouling property of the prepared membranes with four model proteins. Fig. 7 shows the protein adsorptions of four different models on PVF/F127 membranes. Comparing with

Fig. 5, the results of protein adsorption showed the equivalent tendency of antifouling performance. Higher F127 contents in membranes indicate lower deposit quality of foulants and an improved antifouling property. Comparing the results of lysozyme (red line) and catalase (blue line) in Fig. 5 and Fig. 7, it is obvious that lysozyme model is worse than catalase in the antifouling performance for all PVF/F127 membranes. The data of water contact angles and protein adsorptions agreed with AFM force curves very well, which could be an evidence of correctness and effectiveness of AFM force curve method.

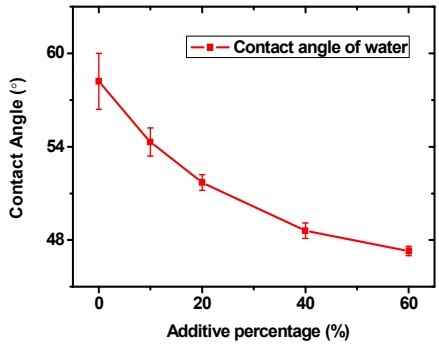

Fig. 6 Water contact angles of PVF/F127 membranes with different ratios.

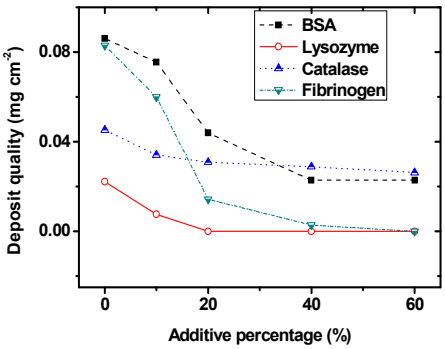

Fig. 7 Protein adsorptions on PVF/F127 membranes with different ratios.

Conclusions

The spring constants of the AFM cantilevers calibrated using electromagnetic balance method have much smaller uncertainties than the ranges provided by the distributers. Through adding the calibration process of AFM cantilevers, adhesion forces between different model proteins and the membranes could be accurately compared. Therefore, the antifouling universality of ultrafiltration membrane can be evaluated and the antifouling performance of different foulants to membrane can be compared using AFM force curves. The comparison experiments results of protein absorption and water contact angle were agreed with AFM force curves very well. Utilizing PVF as the membrane-forming material and F127 as the antifouling additive, the as-prepared membranes have shown better antifouling property for all four foulants, which indicates superior antifouling universality. Among the PVF membranes with different percentages of F127 additive, 60% is the most suitable ratio for a good antifouling performance.

Acknowledgements

This work was supported by '973' project of China [2012CB937500]; National Natural Science Foundation of China [51305298]; and Tianjin Research Program of Application Foundation and Advanced Technology [13JCQNJC04700]. The authors would like to thank Dr. Sen Wu, Mr. Qingchao Chen and Mr. Xinyu Geng for their contribution to the setup of the calibration system.

Notes and references

[a] State Key Laboratory of Precision Measuring Technology and Instruments, Tianjin University, Tianjin 300072, China;
[b] Key Laboratory for Green Chemical Technology of Ministry of Education, College of Chemical Engineering and Technology, Tianjin University, Tianjin 300072, China;
* Author to whom correspondence should be addressed; E-Mail: xulinyan@tju.edu.cn (L.X.) Tel.: +86-186-9806-3909

1. M.A. Shannon, P.W. Bohn, M. Elimelech, J.G. Georgiadis, B.J. Marinas and A.M. Mayes, *Nature*, 2008, **452**, 301.
2. J. Pieracci, J. Crivello and G. Belfort, *J. Membr. Sci.*, 2002, **202**, 1.
3. D. Rana and T. Matsuura, *Chem. Rev.*, 2010, **110**, 2448.
4. A.V.R. Reddy, D.J. Mohan, A.V. Bhattacharya, J. Shah and P.K. Ghosh, *J. Membr. Sci.*, 2003, **214**, 211.
5. J. Pieracci, D.W. Wood, J.V. Crivello and G. Belfort, *Chem. Mater.*, 2000, **12**, 2123.
6. H. Chen and G. Belfort, J. Appl. *Polym. Sci.*, 1999, **72**, 1699.
7. I.C. Kim, J.G. Choi and T.M. Tak, *J. Appl. Polym. Sci.*, 1999, **74**, 2046.
8. J.F. Blanco, J. Sublet, Q.T. Nguyen and P. Schaetzel, *J. Membr. Sci.*, 2006, **283**, 27.
9. L.F. Hancock, S.M. Fagan and M.S. Ziolo, *Biomaterials*, 2000, **21**, 725.
10. J.Y. Park, M.H. Acar, A. Akthakul, W. Kuhlman and A.M. Mayes, *Biomaterials*, 2006, **27**, 856.
11. L. Ying, P. Wang, E.T. Kang and K.G. Neoh, *Macromolecules*, 2002, **35**, 673.
12. Q. Shi, Y. Su, S. Zhu, C. Li, Y. Zhao and Z. Jiang, *J. Membr. Sci.*, 2007, **303**, 204.
13. K. Xiao, X.M. Wang, X. Huang, T.D. Waite and X.H. Wen, *J. Membr. Sci.*, 2011, **373**, 140.
14. G.J. Zhang, S.L. Ji, X. Gao and Z.Z. Liu, *J. Membr. Sci.*, 2008, **309**, 28.
15. K. Gunther, G. Michael, B. Elmar and C. Brunero, *European Polymer Journal*, 2014, **55**, 123.
16. M.A. Ferguson and J.J. Kozlowski, *J. Chem. Educ.*, 2013, **90**, 364.
17. S. Jian, C. Tasi, S. Huang and C. Luo, *Journal of Alloys and Compounds*, 2015, **622**, 601.
18. J. Zhang, Z. Xu, M. Shan, B. Zhou, Y. Li, B. Li, J. Niu and X. Qian, *J. Membr. Sci.*, 2013, **448**, 81.
19. S. Liang, G. Qi, K. Xiao, J. Sun, E.P. Giannelis, X. Huang and M. Elimelech, *J. Membr. Sci.*, 2014, **463**, 94.
20. Z. Xu, J. Zhang, M. Shan, Y. Li, B. Li, J. Niu, B.Zhou and X. Qian, *J. Membr. Sci.*, 2014, **458**, 1.
21. P. Zhang, Y. Wang, Z. Xu and H. Yang, *Desalination*, 2011, **278**, 186.

22. X. Ma, Q. Sun, Y. Su, Y. Wang and Z. Jiang, *Sep. Purif. Technol.*, 2007, **54**, 220.
23. W. Zhao, Y. Su, C. Li, Q. Shi, X. Ning and Z. Jiang, *J. Membr. Sci.*, 2008, **318**, 405.
24. Y. Wang, Y. Su, Q. Sun, X. Ma, X. Ma and Z. Jiang, *J. Membr. Sci.*, 2006, **282**, 44.
25. F. Oesterhelt, D. Oesterhelt, M. Pfeiffer, A. Engel, H.E. Gaub and D.J. Muller, *Science*, 2000, **288**, 143.
26. P. Frederix, P.D. Bosshart and A. Engel, *Biophysical Journal*, 2009, **96**, 329.
27. C.A. Bippes and D.J. Muller, *Rep. Prog. Phys.*, 2011, **74**, 086601.
28. M.S. Kim, J.H. Choi, J.H. Kim and Y.K. Park, *Meas. Sci. Technol.*, 2007, **18**, 3351.
29. Y.P. Song, S. Wu, X.Y. Geng and X. Fu. *Nanotechnology and Precision Engineering*, 2014, **4**, 249.
30. Y.P. Song, S. Wu, L.Y. Xu and X. Fu, *Sensors*, 2015, **15**, 5865.
31. E.C. Cho, D.H. Kim and K. Cho, *Langmuir*, 2008, **24**, 9974.
32. D.G. Kim, H. Kang, S. Han and J.C. Lee, *Journal of Materials Chemistry*, 2012, **22**, 8654.
33. Y. Mo, A. Tiraferri, N.Y. Yip, A. Adout, X. Huang and M. Elimelech, *Environmental Science and Technology*, 2012, **46**, 13253.
34. C.J. Weinman, N. Gunari, S. Krishnan, R. Dong, M.Y. Paik, K.E. Sohn, G.C. Walker, E.J. Kramer, D.A. Fischer and C.K. Ober, *Soft Matter.*, 2010, **6**, 3237.
35. S. Kang, A. Asatekin, A.M. Mayes and M. Elimelech, *Journal of Membrane Science*, 2007, **296**, 42.
36. A. Asatekin, S. Kang, M. Elimelech and A.M. Mayes, *Journal of Membrane Science*, 2007, **298**, 136.
37. Y.Q. Wang, T. Wang and Y.L. Su, *Langmuir*, 2005, **21**, 11856.

